Copyright IPCO-2014
Vol.2
ISSN : 2356-5608

The simulation of InGaN/GaN/AlGaN MSM Photodetector with SILVACO program

Zehor ALLAM[1],Abdelkader HAMDOUNE[2], Chahrazed BOUDAOUD[3],Asmaa AMRANI[4],Aicha SOUFI[5],Zakia NAKOUL[6]
Unity of Research "Materials and Renewable Energies", Faculty of Science, University of Abou-bekr Belkaid, PO Box 230, 13000, Tlemcen, ALGERIA
Phone: 00213-43-28-56-86
Fax: 00213-43-28-56-85
[1]E-mail: zh1344@yahoo.fr

Abstract– In this paper, we consider an InGaN/GaN/AlGaN ultraviolet (UV) photodetector. We first describe internal characteristics.The device exhibited a very good current of about 1.5 mA it was found for -10V applied bias this is in good agreement with the experimental value of current..The variation of photocurrent versus optical wavelength demonstrates a peak of 22.5 µA at a wavelength between 100 nm and 650nm, under -0.2 V bias.

Keywords– *Gallium nitride (GaN), AlGAN, InGaN, UV photodetector.*

I.INTRODUCTION

N-nitride semiconductor materials have recently attracted much interest in applications to optical and electronic devices [1]. Wide band gap materials, especially III-V nitride materials, have attracted extensive interest more and more for their applications in making light emitting devices, high-power and high-temperature electronic devices, and ultraviolet detectors. The use of III-V nitrides for photoelectric detector applications is expected to yield high responsivity with low dark currents over a wide range of temperatures. GaN and A1N have direct band gaps of 3.4 and 6.2 eV, respectively.
Since they are miscible with each other and form a complete series of AlGaN alloys, AlGaN has direct band gaps from 3.4 to 6.2 eV, with corresponding cutoff wavelengths from 365 to 200 nm [2].
MSM photodiodes are comprised of two back-to-back Schottky diodes by using an interdigitated electrode configuration on top of an active light collection region.
This photodetector cannot operate at a zero bias. MSM photodiodes are inherently fast due to their low capacitance per unit area and are usually transit time limited, not time constant limited. With electron beam lithography, the electrode width and spacing can be made with submicron dimension which greatly improves the speed. The biggest drawback of MSM photodetectors is their intrinsic low responsivity. MSM detectors exhibit low photoresponsivity mainly because the metallization for the electrodes shadows the active light collecting region.

In new technologies, the need for high quality materials AlN, GaN, InN and their alloys AlGaN, InGaN is a condition essentially. The basic research is very important to understand the mechanisms of growth and thus improve the quality of materials controlling the growth conditions and also exploring new ways to implement the ability of modern growth [3].

II.MODEL AND STRUCTURAL DESIGN

First of all, basic device model is established based on the nature of GaN, AlGaN and InGaN, and all of the simulated results are on the basis of the drift-diffusion equations.
The proposed structure of InGaN/GaN/AlGaN UV photodetector is shown in Fig. 1; it was simulated using ATHENA and ATLAS in SILVACO TCAD device simulation.

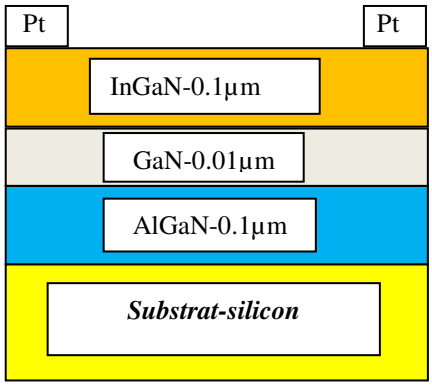

Fig.1. Structure of studied MSM UV photodetector with Pt electrodes.

The relationships between $Al_xGa_{1-x}N$ band gap E_g and the Al components x can be expressed as :

$$E_g(x) = x \times E_g(AlN) + (1-x) \times E_g(GaN) - b \times (1-x) \times x \quad (1)$$

$$E_g(Al_xGa_{1-x}N) = 6.28x + 3.42(1-x) - 1.3\times(1-x)\times x \quad (2)$$

where $E_{g(AlN)}$= 6.2 eV, $E_{g(GaN)}$= 3.39 eV, and b=1 [4].

And the relationship between the band gap energy (Eg) and the indium fraction (x) were proposed using Vegard's Law modified by a bowing parameter (b):

$$E_g(x) = x\times E_g(GaN) + (1-x)\times E_g(InN) - b\times(1-x)\times x \quad (3)$$

Where $Eg._{GaN}$ =3.42 eV; $Eg._{InN}$ = 0.77 eV and b =1.43 eV [5].

The detector is based on a 0.1µm thick AlGaN epitaxial layers grown on sapphire substrate by metalorganic chemical vapor deposition (MOCVD) [6]. The sample InGaN / GaN / AlGaN consisted of a temperature of 0.01 µm thick low (550-C) GaN layer, at 0.1 µm of InGaN thick at high temperature (1050-C) N layer unintentionally doped, a layer 0.1µm thick temperature (1100-C) undoped AlGaN interlayer and 0.3µm thick Silicon. With 250 nm of Pt film was then deposited on the sample by RF magnetron sputtering.

The energy band diagram has been simulated using BLAZE tool, which is interfaced with ATLAS is a general purpose 2-D device simulator for III–V, II–VI materials, and devices with position dependent band structure (i.e., heterojunctions) [3]. BLAZE accounts for the effects of positionally dependent band structure by modifications to the charge transport equations .The net doping of MSM UV photodetector, as shown in Fig.3.

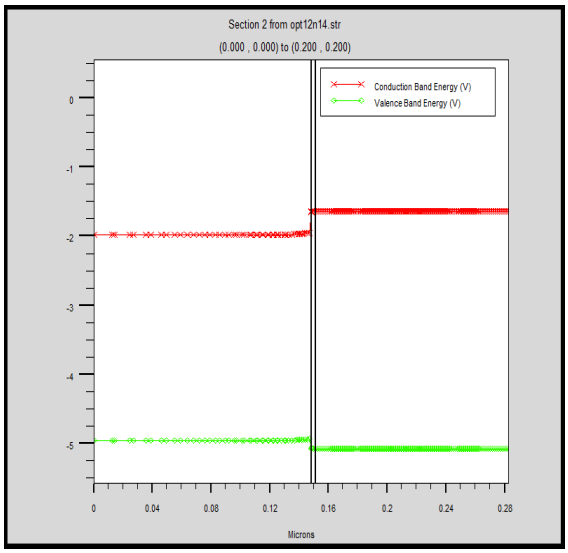

Fig.2. Energy band diagram.

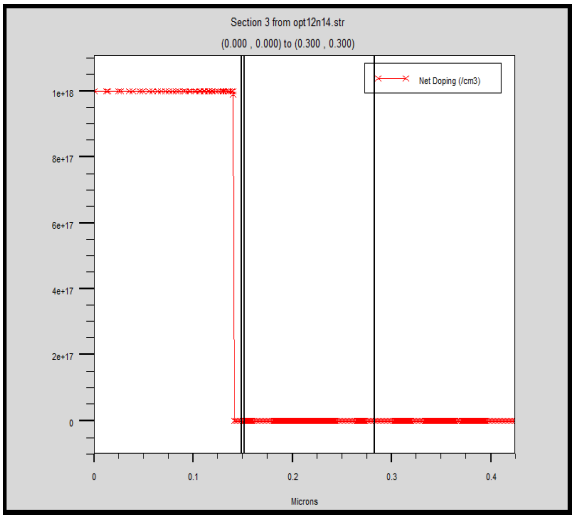

Fig.3.Net doping of InGaN /GaN/AlGaN photodetector.

Doping is a technique that can increase the amount of holes or electrons of a material by substituting a very small amount of its atoms with atoms of a different nature. We doping InGaN layer with n-type the concentration of doping equal $1.10^{-19}cm^{-3}$.We used the method of ion implantation it is technique of doping interesting because it allows precise control of the doping profile. However, it must be followed by an annealing required for the activation of dopants and reduction of disorder induced by implantation [7].

III. RESULTS AND DISCUSSION

A two-dimensional numerical simulation of an InGaN/GaN/AlGaN ultraviolet detector was carried out using ATLAS software. A program was developed separately in DECKBUILD window interfaced with ATLAS for calculating different characteristics of the photo detector. The simulation included the solution of five decoupled equations using Newton iteration method. Carrier and doping densities were calculated using Fermi-Dirac statistics. In calculation of mobility the concentration dependent model was used and for extracting the electrical characteristics, the optical, SRH and Auger recombination processes were taken into account. Different recombination rates are given as:

$$R_c^{opt} = C_c^{opt}(pn - n_i^2) \quad (1)$$

$$R_{SRH} = \frac{pn - n_i^2}{\tau_{pO}\left[n + n_i \times \exp\left(\frac{E_t}{kT}\right)\right] + \tau_{nO}\left[p + n_i \times \exp\left(-\frac{E_t}{kT}\right)\right]} \quad (2)$$

$$R_{Auger} = C_n(pn^2 - nn_i^2) + C_p(p^2 n - pn_i^2) \quad (3)$$

$$R_{surf} = \frac{pn - n_i^2}{\tau_p^{eff}\left[n + n_i \times \exp\left(\frac{E_t}{kT}\right)\right] + \tau_n^{eff}\left[p + n_i \times \exp\left(-\frac{E_t}{kT}\right)\right]} \quad (4)$$

Here C_c^{opt} is the capture rate of carriers; C_n and C_p are Auger coefficients for electrons and holes respectively; n and p are equilibrium electron and hole concentration, E_t is energy level of trap; n_i is intrinsic carrier concentration; τ_{n0} and τ_{p0} are SRH lifetime of electrons and holes respectively; τ_n^{eff} and τ_p^{eff} are effective life times of electrons and holes respectively [8].

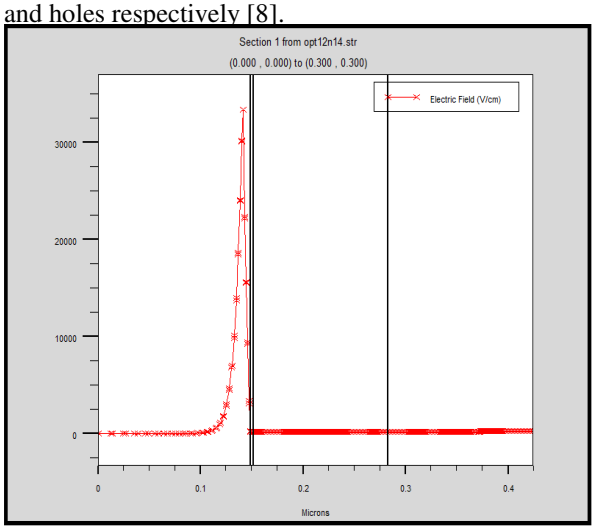

Fig.4. Simulated electric field profile in absence of external biasing.

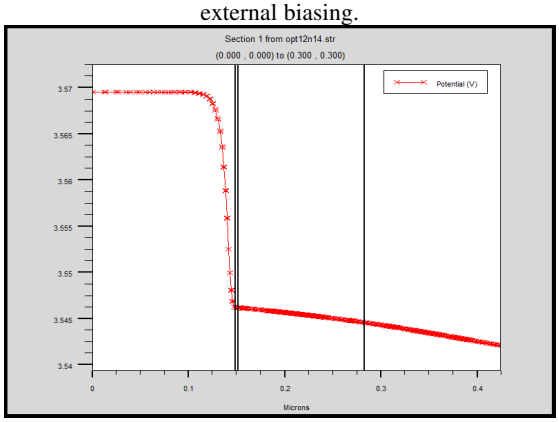

Fig.5. InGaN/GaN/AlGaN internal potential.

The internal polarization-III nitrides have a character piezoelectric. This effect is defined as the creation of an electric field due to a mechanical deformation, and conversely, as the creation of mechanical deformation when applying an electric field to a material. It is due to the lack of symmetry in the crystal structure, the nature of the highly ionic chemical bonds and distortion present in the crystal (due to lattice mismatch between the material and the substrate, for example). The piezoelectric polarization is not necessarily oriented in the same direction as the internal polarization. It depends on the material properties [9].

The electric field and the potential across the structure shown in Fig.4 and Fig.5, confirm the presence of barriers at the interfaces despite an electric field in the largest N-type InGaN, promoting separation of photo-generated carriers. Finally, the carrier concentration through consequently there is a phenomenon of accumulation of electrons at interfaces.This strong field will create a potential barrier for electrons at the interface, as shown in Fig.5.

In the interface metal /semiconductor is a potential barrier for electrons is the difference in work function between the metal and the semiconductor. This causes the formation of heterojunction a potential well in the small-gap material in which electrons from the donor layer are transferred and accumulated. The heterojunction is characterized by the discontinuity of the energy of the conduction band between the two materials, plus the value of the energy of the conduction band is high, the electron transfer from the donor layer to the channel will be better In addition, over the material of the channel will be small gap, the transport properties (speed, mobility) will be better.

The simulated current density is shown in Fig.6. We observe a high value of current density in the layer InGaN : 0.215 A/cm^2 for reverse bias up to 0.5 V.

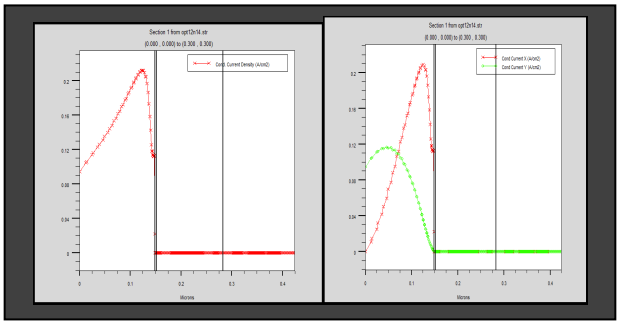

Fig.6. Conduction current density.

The photodetector has the smallest gap, has the highest current density. Indeed, because of its low gap, most of the photons arriving at the photodetector are based InGaN have energy equal to or greater than the gap producing a high current density. When the gap increases, the voltage increases but also fewer photons have sufficient energy to be absorbed, reducing the current density of photodetector.

The mechanism of optical gain in InGaN quantum wells of UV photodetector real is not yet fully understood. It can be strongly affected by non-uniform distribution. Internal bias fields tend to separate quantum confined electrons and holes, which reduces the optical gain and spontaneous emission. However, the screening of the electrons and holes are provided to remove bias fields at high current operation [10].

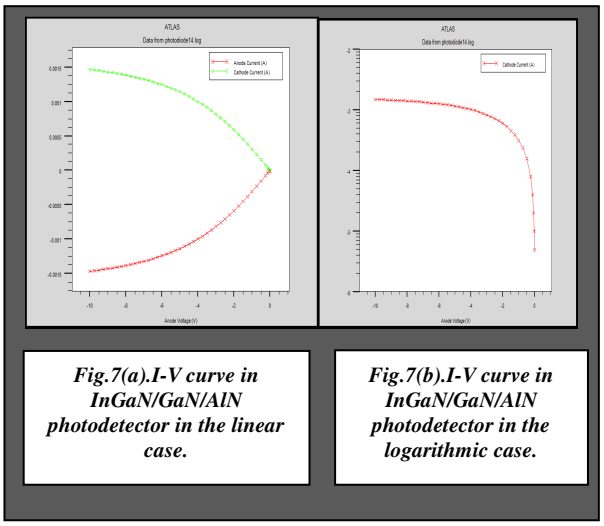

Fig.7(a).I-V curve in InGaN/GaN/AlN photodetector in the linear case.

Fig.7(b).I-V curve in InGaN/GaN/AlN photodetector in the logarithmic case.

Fig.7.I-V curve in InGaN/GaN/AlN photodetector.

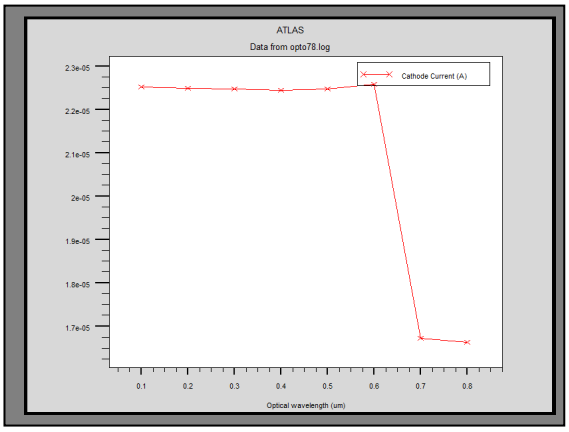

Fig.8. Photocurrent as a function of optical wavelength, for -0.5V.

A Schottkey Contact is formed between the InGaN and Au metal determined by the I-V curve measured between Au and InGaN. Also it is confirmed by Electron Beam induced current measurements. The diode has an apparently rectifying current characteristic.

Fig. 8 shows I–V characteristics of the simulated InGaN/GaN photodetector.

We find a current of about 1.5 mA it was found for -10V applied bias this is in good agreement with the experimental value of current.

The variation of photocurrent of InGaN/GaN/AlGaN photodetector as a function of wavelength at a bias voltage of -0.2V is shown in Fig.8. We can optimize the performance of the device by changing the doping concentration and dimensions of the device for high bandwidth performance.

This structure provides a spectral response broadband UV and visible range. It is particularly suitable for applications in the ultraviolet and visible from 100 nm to 650 nm with a peak current equal $2.25.10^{-5}$A is a good result it is possible that good performance because the use of InGaN and the substrate silicon in the structure of photodetector.

VI.CONCLUSION

In this paper, we studied an InGaN/GaN/AlGaN photodetector device. Modeling and simulation were performed by using ATLAS-TCAD simulator. Energy band diagram, conduction current density, internal potential and electric field were performed.

The device exhibited a very good current of about 1.5mA.The variation of photocurrent versus optical wavelength demonstrates a peak of 22.5 µA at a wavelength between 100 nm and 650nm, under -0.2 V bias.

The simulation and modeling described in this work can be used for optimizing the existing ultraviolet detectors and developing new devices.

REFERENCES

[1] Ping-Chuan Chang, Chin-Hsiang Chen , Shoou-Jinn Chang , Yan-Kuin Su, Chia-Lin Yu, Bohr-Ran Huang, Po-Chang Chen, High UV/visible rejection contrast AlGaN/GaN MIS photodetectors, Thin Solid Films 498 (2006)133 – 136.

[2] Reine M B, Hairston A, Lamarre P, et al. Solar-blind AlGaN 256×256 p-i-n detectors and focal plane arrays. Proc SPIE,2006, 6119,pp1-15.

[3] Pierre Masri, "Silicon carbide and silicon carbide-based structures, the physics of epitaxy", Surface Science Reports 48 (2002), pp. 1–51.

[4] D. L. Pulfrey and B. D. Nener, "Suggestions for the development of GaN-based photodiodes," *Solid-State Electronics.* vol. 42, no. 9, pp. 1731-1736, Mar. 1998.

[5] J. Wu, W. Walukiewicz, K.M. Yu, J.W. Ager III, E.E. Haller, H. Lu, W.J. Schaff, "Small band gap bowing in In1-xGax/N alloys," Appl. Phys. Lett(2002). pp. 4741-4743.

[6] Guozhen SHEN, Di CHEN, "One-dimensional nanostructures for electronic and optoelectronic devices", Front. Optoelectron. China 2010, 3(2):.pp.125–138.

[7] Katsikini, M., et al. Raman study of Mg, Si, O, and N implanted GaN. Journal of Applied Physics.2003, Vol. 94, 4389.

[8] A.D.D. Dwivedi, A. Mittal, A. Agrawal, and P. Chakrabarti, "Analytical modeling and ATLAS simulation of N+-InP/n0-In0.53Ga0.47As/p+-In0.53Ga0.47As p-i-n photodetector for optical fiber communication", Infrared Physics & Technology 53 (2010), pp. 236–245.

[9]Liu, L. and Edgar, J.H. Substrates for gallium nitride epitaxy. Materials Science and Engineering R.2002, Vol. 37, 61.

[10]DMITRIEV, A.V., and ORUZHEINIKOV, A.L.: 'The rate of radiative recombination in the nitride semiconductors and alloys".MRS Internet J. Nitride Semicond. Res., 1996, 1, pp. 46.